Bull. Mater. Sci. (2019) 42:235
https://doi.org/10.1007/s12034-019-1914-1

Promotion of bone repair of rabbit tibia defects induced by scaffolds of P(VDF-TrFE)/$BaTiO_3$ composites

R GIMENES[1,*], M A ZAGHETE[2], M ESPANHOL[1], D SACHS[1] and M R A SILVA[1]
[1]Institute of Physics and Chemistry, Federal University of Itajubá, Pinheirinho, Itajubá, Minas Gerais 37500-003, Brazil
[2]Chemistry Institute, UNESP, Quitandinha, Araraquara, SP 14800-900, Brazil
*Author for correspondence (rossano@unifei.edu.br)

MS received 18 September 2018; accepted 16 April 2019

Abstract. In this work, scaffolds made of a novel experimental 0–3 type composite were implanted onto non-critical defects in rabbit tibiae. This work discusses the bone repair promoted by polyvinylidene fluoride-trifluoroethylene P(VDF-TrFE)/barium titanate ($BaTiO_3$) composite that scaffolds with 10 vol% $BaTiO_3$. Prior to implant surgery, the P(VDF-TrFE)/$BaTiO_3$ scaffolds, moulded into a membrane disk, were subjected to a cytotoxicity test (ASTM F895-84). A standardized transverse osteotomy was made with the following dimensions: 4.5 mm in width by 9 mm in length, at the proximal tibial metaphysis, in adult male rabbits, by using a cylindrical drill, cooled with a physiologic solution. These critical defects were filled with blood clot on the left tibiae (control group), whereas the right tibiae were covered with composite scaffolds, measuring 5 mm in thickness and 10 mm in diameter (experimental group); $n = 12$ for each group. After 21 days, the rabbits were sacrificed and the tibiae bone fragments were conducted to demineralization routines, from fixation and stain procedures to histological analysis. The scaffolds promote the growth of the bone, resulting in an increased repair with callus formation around the scaffold and high mitotic activity at newly formed bones.

Keywords. Scaffolds; bone repair; P(VDF-TrFE)/$BaTiO_3$ composites.

1. Introduction

The importance of natural piezoelectric phenomena on bone growth and maintenance has been known. Electrical potentials are generated by the collagen fibres and hydroxyapatite crystals, due to piezoelectricity of these extracellular components, as response to mechanical load [1,2].

The influence of electrical stimulation on bone healing is established and it has been demonstrated that the application of electrical or mechanical stimuli can enhance or stimulate osteogenic activities [3]. Therefore, the addition of a piezo or electrically active components to an allogeneic material, implanted on a bone defect, would enhance the healing of such bones.

Since the pioneer work was developed by Fukada *et al* [4], who observed the callus formation around a polarized electret material implanted on rabbits' femurs, significant development has been established in the electroactive implant field, such as bioceramics [5], piezoelectric polymers [6] and piezoelectric composites [7–10]. Among the piezoelectric polymers, PVDF and its copolymers, such as polyvinylidene fluoride-trifluoroethylene (P(VDF-TrFE)) are the most employed in bone regeneration due to noted biocompatibility with several cell extracts [8–15].

Barium titanate ($BaTiO_3$), a ferroelectric ceramic, has been shown to be biocompatible *in vitro* and *in vivo* studies [5], and several studies have indicated the potential benefits of $BaTiO_3$-based materials as implants. Jianqing *et al* [16] used a barium titanate-hydroxyapatite (HABT) piezoelectric composite for bone graft, and observed through histological analysis, improvement in the bone tissue growth on HABT samples, when compared to HA controls. An *in vitro* study of osteoblast-like cells, cultured on poled and unpoled HABT ceramics, demonstrated cell proliferation on intimate contact with the material, evidencing the biocompatibility *in vitro* of this material [5]. Zanfir *et al* [17] studied a collagen-HA/BT composite and attributed the excellent *in vitro* osteoinductive properties to the ferromagnetic properties of $BaTiO_3$.

The biocompatibility *in vitro* of P(VDF-TrFE)/$BaTiO_3$ composites was demonstrated by the results previously published: experiments with human osteoblastic cells, cultured on membranes of the composite P(VDF-TrFE)/$BaTiO_3$, showed bone-like nodule formation. This behaviour was not observed in the control group (e-PTFE periodontal membranes) [8].

Real-time polymerase chain reaction experiments revealed high expression of phenotypic markers of fibroblasts from human periodontal ligament (hPDLF), keratinocytes, as well as a great expression of apoptotic genes in cultures grown under P(VDF-TrFE)/$BaTiO_3$, when compared with e-PTFE membranes [18]. We also observed that osteoblastic cells, cultured under P(VDF-TrFE)/$BaTiO_3$, exhibited a significantly higher mRNA expression, compared to cells cultured under commercial e-PTFE for the following markers of the osteoblastic phenotype: RUNX2, type I collagen, osteopontin,

Published online: 19 July 2019

alkaline phosphatase, bone sialoprotein, osteocalcin and for markers associated with the control of the apoptotic cell death: Bcl2-associated X protein and survivin [19]. Recently, an *in vivo* study demonstrated that osteoblastic cells from bone marrow, combined with the PVDF-TrFE/$BaTiO_3$ membrane, increased the bone formation [20].

In the field of tissue engineering, the possibility to create active or smart scaffolds not only provide mechanical support, but also activate the cell proliferation, is very promising. Damaraju *et al* [13] verified the attachment of human mesenchymal stem cells on the fibres of a PVDF scaffold. Larger alkaline phosphatase activity and early mineralization of cell cultured on a PVDF scaffold were observed, when compared to the control. Randomly oriented and aligned electroactive fibrous scaffolds, made of poly-(L-lactic acid)/$BaTiO_3$, promoted polygonal spreading and encouraged early osteogenic differentiation of bone marrow mesenchymal stem cells [21].

Considering these findings, we hypothesize that scaffolds made of P(VDF-TrFE)/$BaTiO_3$ can promote bone formation. Then, the present work reports an investigation on the use of composite P(VDF-TrFE)/$BaTiO_3$ scaffolds, implanted in tibiae defects in rabbits.

2. Experimental

2.1 *Materials*

The P(VDF-TrFE) copolymer was supplied by Piezotec S.A. (Saint Louis, France). It consists of a random copolymer of 80 mol% VDF and 20 mol% TrFE. Barium titanate powder ($BaTiO_3$) was supplied by Aldrich. Commercial $BaTiO_3$ powder was sintered at 1380°C for 5 h to obtain a very strong agglomerate that was milled using a planetary ball mill (Nuoya, China) for 2 h in agate jars and isopropanol medium.

2.2 *Fabrication of P(VDF-TrFE)/$BaTiO_3$ scaffolds*

The P(VDF-TrFE)/$BaTiO_3$ composites with 10 vol% $BaTiO_3$ composites were obtained by dissolving the PVDF-TrFE pellets as received in dimethyl formamide (DMF) at 50°C using a polymer/solvent ratio of 15 g/100 ml. $BaTiO_3$ powder was added to the polymer solution and homogenized by using a magnetic stirrer. The viscous precursor dispersion obtained was placed inside a special 5 ml-glass capsule with an inlet for gases at the bottom. Water was sprayed inside the composite precursor dispersion using nitrogen as the carrier gas. The sprayer employed was a domestic ultrasonic nebulizer with a 130 W power and the inlet gas flow was adjusted to 200 cm^3 min^{-1}. After 30 min, a porous scaffold composite was obtained, removed from the capsule, dried under vacuum at 90°C for 12 h and then, cut into disks measuring 10 mm in diameter and 1.5 mm in thickness.

The scaffold's porosity is created and controlled by the inlet flow of sprayed water, in the dispersion of PVDF-TrFE/DMF/$BaTiO_3$, due to difference in the component solubility. The solubility in water of DMF is higher than that of the PVDF-TrFE. In this way, when water is sprayed through the dispersion, its solvent is removed by water bubbles. After the precursor dries, the air bubbles trapped inside make the precursor become a porous solid foam.

2.3 *Characterization of scaffolds*

2.3a *Morphology by scanning electron microscopy (SEM)*: Composite constructs were frozen with liquid nitrogen and sectioned at cross-sections. The slices were coated with gold, using a sputter machine (Shimadzu, Japan). Their morphologies were examined by a SEM (SS500, Shimadzu, Japan), using images of backscattered electrons. The pore size was calculated from SEM images by selecting five arbitrary areas measured.

2.3b *Open porosity*: The open porosity was calculated by the Archimedes method. Scaffold fragments measuring 1.00 ± 0.03 cm^3 were weighed (dry weight) and then submerged in ethanol within a 20 ml glass syringe. The piston was pressed and released multiple successive times to force the liquid into the pores. After filling the open pores with ethanol, the scaffold fragments were removed from the syringe and placed in an Archimedes apparatus to measure the wet and suspended weight.

The open porosities (ϕ) were calculated using the following equation:

$$\phi = \frac{W_{\text{wet}} - W_{\text{dry}}}{W_{\text{wet}} W_{\text{suspended}}}. \quad (1)$$

2.3c *Scaffold composite poling*: Scaffold disks measuring 10 mm in diameter and 1.5 mm in thickness were poled in a vacuum (10^{-4} torr), at room temperature, using a direct current voltage source with an electric field of 25 MV m^{-1} at 90°C for 30 min. Electrodes made of conductive rubber were used in this process, because they can be easily removed to avoid unsatisfactory *in vivo* reactions. The piezoelectricity of P(VDF-TrFE)/$BaTiO_3$ composites was measured using a Berlincourt d_{33} Meter (APC International, Mackeyville, PA, USA), 24 h after the poling process.

2.3d *Cytotoxicity assay (ASTM F895-84 rev 2011)*: Scaffold disks measuring 9 mm in diameter were placed into a 24-well plate. The derived cells from mouse connective tissue—NCTC clone 929 (CCL1, ATCC, USA)—were seeded into wells at a 2×10^4 cell per well density. These cells were cultured in α-minimum essentials medium (Gibco, USA), supplemented with 10% of bovine serum, L-glutamine, 50 μg ml^{-1} gentamicin (Gibco, USA), 0.3 μg ml^{-1} fungizone (Gibco, USA) and 1×10^{-7} M dexamethasone (Sigma,

USA). The cells were incubated at 37°C in a humidified atmosphere with 5% CO_2 for 48 h. The medium was substituted by neutral red agar and incubated at 37°C for 24 h. The USP negative control plastic reference standard was employed as the negative control group, and phenol solution as the positive control group. The medium containing a vital stain shall discolour, if the P(VDF-TrFE)/$BaTiO_3$ scaffolds are tested and proven to be toxic or if they deliver any toxic compound.

2.3e *In vivo experiments*: Rectangular scaffold fragments measuring 4.5 × 9.0 and 1.5 mm in thickness were implanted in rabbits' tibiae. During surgery, the animal was placed on a left lateral decubitus position and under general anaesthesia using 0.35 ml kg^{-1} ketamine chlorhydrate (Francotar, Virbac, Brazil) and 0.25 ml kg^{-1} xylazine chlorhydrate (Virbaxyl, Virbac, Brazil). The legs were shaved and then sprayed with an antiseptic solution. A 3 cm rectilinear incision was made at the anterior face, under the tibia tuberosity at the distal end of the tibia. The adjacent conjunctive tissue was folded using a scalpel, exposing the bone. The periosteum was incised, and a standardized transverse tibial osteotomy was performed to produce the critical size defects (CSDs). A CSD of ∼4.5 mm in width and 9 mm in length was surgically drilled at the proximal tibial metaphysis; it was made by using a drill, cooled with a physiological solution. At the left tibia osteotomy, a flexible scaffold composite was placed around the cortical bone under the periosteum (experimental group). At the right tibiae osteotomy, no material was implanted (control group), and the periosteum was repositioned. All animals received an analgesic and anti-inflammatory medication during the post-operative period. Radiological observation was made on the 1st and 21st days of post-surgery.

Twenty-one days later, the animals were sacrificed after being deeply sedated. Fragments of tibiae were removed and cut in a longitudinal direction into thin serial sections with a thickness of 0.7 μm, using a microtome. For histological analysis, the samples were stained with hematoxylin–eosin. A Zeiss Axioskop light microscope (Carl Zeiss, Germany) was used for histological analysis.

3. Results and discussion

3.1 *Piezoelectricity of P(VDF-TrFE)/$BaTiO_3$ composite*

The piezoelectric charge coefficient, d_{33}, of the composites ranged from 0.1 to −15.5 pC N^{-1}. The best value of piezoelectricity coefficient, d_{33} (−15.5 pC N^{-1}) was obtained for the composite with 10 vol% $BaTiO_3$. Due to this result, the composition containing 10 vol% $BaTiO_3$ was employed in scaffolds for *in vivo* and *in vitro* experiments. The piezoelectric coefficient d_{33} of the copolymer and ceramic phases has opposite signs. The d_{33} coefficient of PVDF-TrFE is negative because domain walls contract when electric energy is applied through this material. However, for $BaTiO_3$ ceramics, the d_{33} coefficient is positive because the electric energy causes stretching of the crystal and, consequently, deformation. The fact that the composite P(VDF-TrFE)/$BaTiO_3$ with 10 vol% $BaTiO_3$ exhibited a negative d_{33} coefficient indicates that the piezoelectricity of the copolymer prevails over the ceramic piezoelectricity.

The narrow particle size distribution of $BaTiO_3$ powders, milled using a planetary ball mill, reveals an average grain size of 450 nm. This particle size results in a greater piezoelectric effect because, for a piezoelectric composite based on PVDF/$BaTiO_3$, the poling efficiency is higher for particles between 200 and 600 nm [22].

3.2 *Scaffold morphology*

The morphology of the scaffolds can be observed in figure 1A. By analysing the morphology of scaffolds, a porous structure was observed with enough space for blood circulation and cell growth as required for bone scaffolds. Three-dimensional inter-connected porous structure was evidenced. The pores present in the microstructure are open with the pore size ranging from 400 to 550 μm (macropores) and smaller pores ranging from 50 to 100 μm. The macropore walls were formed by solvent evaporation during the drying process. No segregated phase was observed, indicating the good homogeneity of the composites. Figure 1B shows the porosity of the P(VDF-TrFE)/$BaTiO_3$ scaffolds by varying the flow rate of sprayed water injected in the precursor solution. The results indicate that the porosity of the scaffolds increases with the flow rate until 200 cm^3 min^{-1}, and the best obtained porosity value was 79.8 ± 2.1. An increase in the flow rate contributes to generate bubbling in the composite precursor solution. At a high sprayed-water flow rate, the bubbles formed were rich in water, and then the extraction of the solvent DMF was more efficient than at low flow rates. It allowed the growth of pores because, with a rapid extraction of the solvent, the pore walls became rigid enough to support a porous structure. At a 250 cm^3 min^{-1} flow rate, the speed of exhaust gases was higher than the necessary speed to remove the solvent in the bubbles.

3.3 *Callus area and histological analysis*

In figure 2B, both the fracture gap caused by the CSD and the scaffold surrounding the cortical bone under the fracture gap (indicated by arrows) are clearly seen. The approach to attach the scaffolds under the periosteum was adopted to allow good fixation of the scaffold to the cortical bone and to avoid micro-movements, since it could cause leakage of blood clotting. Furthermore, the mechanical interaction between the surrounding tissues and scaffolds depends on the mechanical stability of the scaffold implanted.

Analysing the radiographs taken 21 days after the surgery (figure 2A), a slight thickening of fibrous tissue is observed in the osteotomy, evidencing no bone repair process, as expected, since the CSD model was adopted.

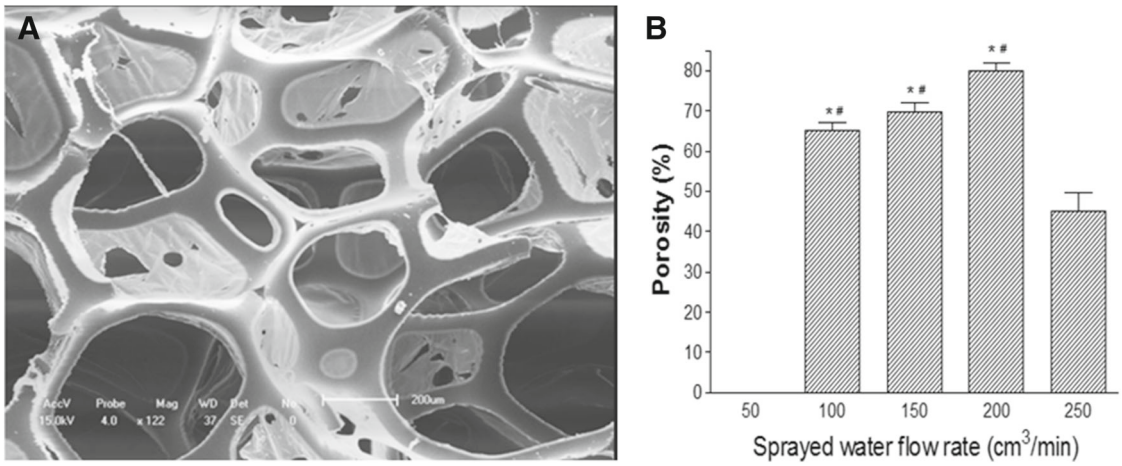

Figure 1. (**A**) Morphology of P(VDF-TrFE)/$BaTiO_3$ with 10 vol% of $BaTiO_3$ scaffolds observed by SEM image and (**B**) porosity of the P(VDF-TrFE)/$BaTiO_3$ scaffold obtained with different sprayed-water flow rates.

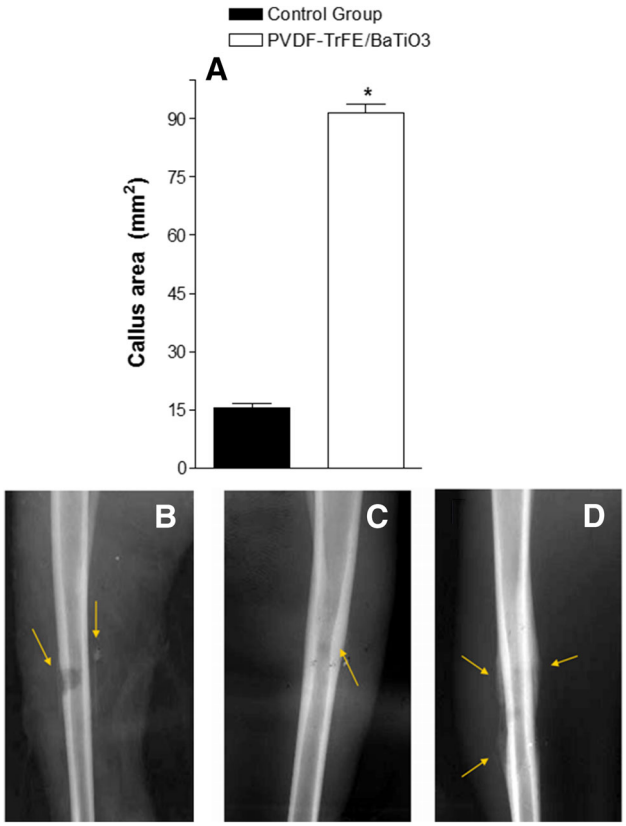

Figure 2. (**A**) Callus area surrounding the fracture gap measured 21 days after surgery by radiographs, (**B**) radiograph of right tibiae (control group) taken 21 days after surgery and (**C**) radiograph of left tibiae that received the composite scaffold taken 21 days after surgery. *Indicates statistically significant difference ($P \leq 0.05$).

The formation of an exacerbated callus is observed around the P(VDF-TrFE)/$BaTiO_3$ scaffolds implanted (figure 2C), and not only under the osteotomy (indicated by two arrows). Considering that this callus was observed around the borders of the scaffolds, it strongly suggests that the P(VDF-TrFE) $BaTiO_3$ scaffolds induced the callus formation. The callus area is higher for the experimental group with scaffolds implanted than the control group (figure 2A). The difference in the callus area between the two groups was statistically significant ($P = 0.003$): 88.6 ± 7.8 mm^2 for the experimental group and 19.8 ± 7.4 mm^2 for the control group. In figure 2B, the gap is not observed, indicating that the CSD was filled by new bones. The CSD model establishes intraosseous wound in the bone with a critical size, according to the species of the animal, which will not heal spontaneously. The critical size defect model mimics the clinical situations in which a substantial amount of bone is lost due to trauma, infection or tumour [23,24].

By histological observation, figure 3, neo-formed bone filling the CSD is observed in the animals with P(VDF-TrFE)/$BaTiO_3$ scaffolds (figure 3A and B). These results indicate bone regeneration in the osteotomy region. Histological analysis of the control group reveals only old bone and the gap evidence at the CSD site. Analysing figure 3C and D, it is possible to note three different regions in the experimental group. In the margin of the bone defect (figure 3D), the old bone is observed in contact with the neo-formed bone and red blood cells are seen in lacuna. Different tissue morphologies are observed near the opposite margin of the bone defect (region 3), which was in contact with the scaffold. This region corresponds to the external bone callus surface. In areas that were in contact with scaffolds, high growth of bone tissue is found due to high mitotic activity, evidenced by the presence of various nuclei and vascular neo-formation. When neo-bone formation in the control group is compared with the group with scaffolds implanted, high mitotic activity in the tissue surrounded by the scaffolds is evident. The angiogenesis process was also observed in the presence of red blood cells, indicating that the bone repair process is faster in the defects covered with scaffolds. Additionally, inflammatory cells were

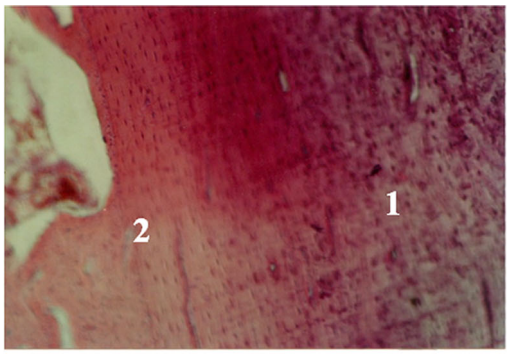

A

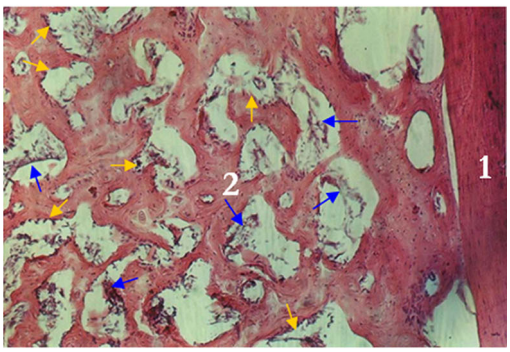

B

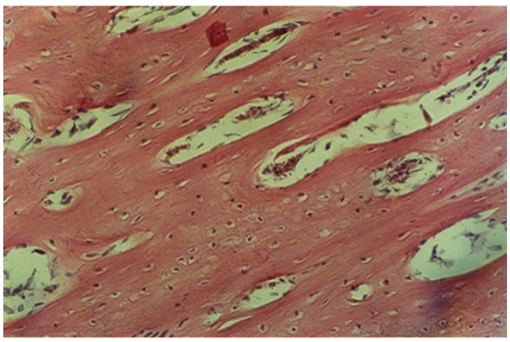

C

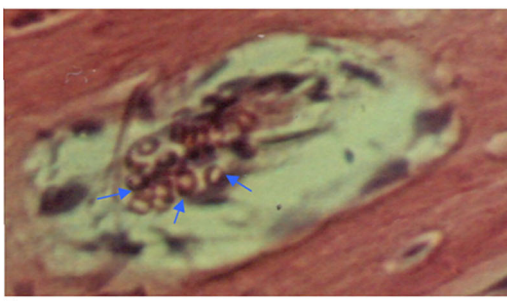

D

Figure 3. Histological sections stained with eosin–hematoxylin observed by inverted light microscopy of the defect site of rabbit tibiae, 21 days following the implantation. Control group: (**A**) neo-bone formation. (**B** and **C**) Histological sections of the group with the composite scaffold implanted showing new bone formation, (**D**) interface neo-formed bone and old bone; (*) collagen fibres near the opposite margin of the bone defect that was in contact with the composite scaffold; arrows: vascular neo-formation. Bar: 50 μm.

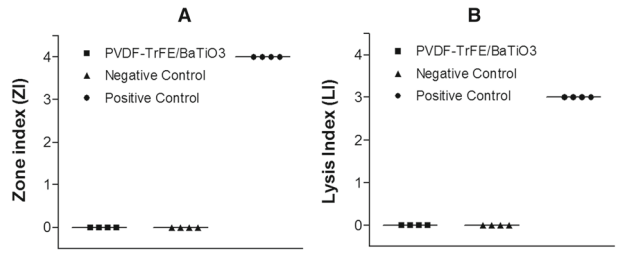

Figure 4. Cytotoxicity assay: zone and lysis indices of NCTC clone 929 connective cells cultured under P(VDF-TrFE)/$BaTiO_3$ scaffolds, USP negative control plastic reference standard and phenol solution (positive control). Cells incubated at 37°C in agar medium with red neutral. The test was made in quadruplicates. Zone index (ZI): 0 means no detectable zone around or under specimen; 4 means zone extends >1 cm beyond the specimen, but does not involve the entire dish; lysis index (LI): 0 means no observable cytotoxicity; 3 means 40–59% of zone affected.

not observed in histological sections, indicating the excellent biocompatibility of P(VDF-TrFE)/$BaTiO_3$ scaffolds.

3.4 *Analysis of cytotoxicity*

Microscopic examination of the fibroblasts cultured under P(VDF-TrFE)/$BaTiO_3$ scaffolds indicates no cell malformation, degeneration, sloughing or lysis of these cells. The following cytotoxicity assay procedure (ASTM F895-84 rev 2011) determined the zone index, which measures the clear zone in which cells do not stain with neutral red and the lysis index which measures the number of cells affected within the zone of toxicity. The results of these indices are presented in figure 4. Analysing these data, it is found that P(VDF-TrFE)/$BaTiO_3$ scaffolds are not cytotoxic to cellular lineage employed since the zone and lysis index are the same as the USP plastic, used as the negative control.

4. Conclusions

The P(VDF-TrFE)/$BaTiO_3$ piezoelectric composite scaffolds were successfully obtained. This material does not present any cytotoxicity, verified by the ASTM F895-84 standard-test method. Implanted in non-critical defects of rabbit tibiae, the callus formation around scaffolds and the high mitotic activity was evidenced and suggest that osteogenesis promotion was mediated by an electrical current generated by piezoelectricity. Considering these findings, we can conclude that P(VF-TrFE)/$BaTiO_3$ with 10 vol% of $BaTiO_3$ scaffolds have the potential to induce bone repair.

Acknowledgements

We would like to thank the Research and Support Foundation of Minas Gerais (FAPEMIG), Grant TEC-APQ-03013-15.

References

[1] Zhang Y, Gandhi A A, Zeglinski J, Gregor M and Tofail S A M 2012 *IEEE Trans. Dielectr. Electr. Insul.* **19** 1151

[2] Hastings G W and Mahmud F A 1991 *J. Mater. Sci. Mater. Med.* **2** 118

[3] Ghiasi M S, Chen J, Vaziri A, Rodrigues E K and Nazarian A 2017 *J. Bone Rep.* **6** 87

[4] Fukada E, Takamatsu T and Yasuda I 1975 *Jpn. J. Appl. Phys.* **14** 2079

[5] Baxter F R, Bower C R, Turner I G and Dent A C 2010 *Ann. Biomed. Eng.* **38** 2079

[6] Ribeiro C, Sencadas V, Correia D M and Lanceros-Méndez S 2015 *Colloids Surf. B Biointerfaces* **136** 46

[7] Bolbasov E N, Popkov D A, Popkov E N, Gorbach E N, Khlusov I A, Golovkin A S *et al* 2017 *Mater. Sci. Eng. C: Mater. Biol. Appl.* **75** 207

[8] Beloti M M, de Oliveira P T, Gimenes R, Zaghete M A, Bertolini M J and Rosa A L 2006 *J. Biomed. Mater. Res. A* **79** 282

[9] Lopes H B, Santos T S, de Oliveira F S, Freitas G P, de Almeida A L, Gimenes R *et al* 2014 *J. Biomater. Appl.* **29** 104

[10] Scalize P H, Bombonato-Prado K F, de Sousa L G, Rosa A L, Beloti M M, Semprini M *et al* 2016 *J. Mater. Sci.: Mater. Med.* **28** 180

[11] Pärssinen J, Hammarén H, Rahikainen R, Sencadas V, Ribeiro C, Vanhatupa S *et al* 2015 *J. Biomed. Mater. Res.* **103** 919

[12] Frias C, Reis J, Capela e Silva F, Potes J, Simões J and Marques A T 2010 *J. Biomech.* **43** 1061

[13] Damaraju S M, Wu S, Jaffe M and Arinzeh T L 2013 *Biomed. Mater.* **8** 1

[14] Martins P M, Ribeiro S, Ribeiro C, Sencadas V, Gomes A C, Gama F M *et al* 2013 *RSC Adv.* **3** 17938

[15] Young T-H, Chang H-H, Lin D-J and Cheng L-P 2010 *J. Membr. Sci.* **350** 32

[16] Jianqing F, Huipin Y and Xingdong Z 1997 *Biomaterials* **18** 1531

[17] Zanfir V, Voicu G, Busuioc C, Jinga S I, Albu M G and Iordache F 2016 *Mater. Sci. Eng. C: Mater. Biol. Appl.* **62** 795

[18] Teixeira L N, Crippa G E, Trabuco A C, Gimenes R, Zaghete M A, Palioto D B *et al* 2010 *Acta Biomater.* **6** 979

[19] Teixeira L N, Crippa G E, Gimenes R, Zaghete M A, de Oliveira P T, Rosa A L *et al* 2011 *J. Mater. Sci.: Mater. Med.* **22** 151

[20] Freitas G P, Lopes H B, Almeida A L G, Abuna R P F, Gimenes R, Souza L E B *et al* 2017 *Calcif. Tissue Int.* **101** 312

[21] Li Y, Dai X, Bai Y, Liu Y, Wang Y, Liu O *et al* 2017 *Int. J. Nanomed.* **12** 4007

[22] Hsiang H-I, Lin K-Y, Yen F-S and Hwang C-Y 2001 *J. Mater. Sci.* **36** 3809

[23] Seman C, Zarida C N, Zamzuri Z, Sharifudin M A, Ahmad A C, Awang M S *et al* 2018 *Int. Med. J. Malays.* **17** 13

[24] Zhao M-D, Huang J-S, Zhang X-C, Gui K-K, Xiong M, Yin W-P *et al* 2016 *PLoS One* **11** 1